Supporting Information for

Electrochemical (De)Lithiation of 1D Sulfur Chains in Li–S Batteries: A Model System Study

Chun-Peng Yang,[†,‡] Ya-Xia Yin,[†] Yu-Guo Guo,*[,†] and Li-Jun Wan*[,†]

[†] CAS Key Laboratory of Molecular Nanostructure and Nanotechnology, and Beijing National Laboratory for Molecular Sciences, Institute of Chemistry, Chinese Academy of Sciences (CAS), Beijing 100190, P. R. China

[‡] University of Chinese Academy of Sciences, Beijing 100049, P. R. China

* To whom correspondence should be addressed. E-mail: ygguo@iccas.ac.cn (Y.-G. G.); wanlijun@iccas.ac.cn (L.-J. W.)

Experimental Section

Synthesis of S/CNTs

CNTs (Nanjing XFNANO Materials Tech Co. Ltd.) were first heated at 450 °C in a dry air flow for 1 h to remove the terminating caps of CNTs prior to use. The open-ended CNTs were milled with S (Singma Aldrich) and pressed into a pellet. The pellet was sealed in a glass tube *in vacuo* and then calcined at 600 °C for 48 h. The as-obtained sample was milled again and then washed with CS_2 to remove the S outside the CNTs. The final S/CNTs were obtained by centrifugation and drying in an oven.

Characterizations

X-ray powder diffraction (XRD) profiles of the samples were collected on a Rigaku D/max-2500 with Cu Kα radiation (λ = 1.54056 Å) at a scan rate of 0.1 °/min. Raman measurements were performed using a DXR micro-Raman spectrometer (Thermo Scientific) with 532 nm excitation laser. Transmission electron microscopy (TEM) images, scanning transmission electron microscopy (STEM) images and the elemental distribution of S/CNTs were observed on JEM-2100F (JEOL) coupled with an energy dispersive X-ray (EDX) spectrometer. SEM images were observed on JEM-6700F (JEOL) with an EDX spectrometer. The content of S in S/CNTs was determined by Ba^{2+} titration using Flash EA 1112. Elemental analysis was also performed on an Electron Probe Microanalyser (EPMA, JEOL JXA-8500F) with four wavelength dispersive X-ray (WDX) spectrometers.

The elemental information was obtained by X-ray photoelectron spectroscopy (XPS) performed on the ESCALab 250Xi (Thermo Scientific) using 200 W monochromatized Al Kα radiation. Data of XPS binding energy are calibrated based on the hydrocarbon C 1s line at 284.5 eV from adventitious carbon. Spectra were fitted with Lorentzian-Gaussian functions and smart background using Thermo Avantage software.

Electrochemistry

The electrode materials, S/CNTs (or empty CNTs for comparison) and poly(vinyl difluoride) binder with a weight ratio of 85:15, were mixed as slurry in N-methyl-2-pyrrolidone (NMP), coated onto an Al foil, and further dried at 60 °C overnight. Two-electrode Swagelok-type batteries were assembled in an argon-filled glove box for evaluating the electrochemical properties in an argon-filled glove box (oxygen and moisture lower than 0.1 ppm), using glass fiber from Whatman as the separator and lithium foil as the anode. The electrolyte was 1 M lithium bis(trifluoromethanesulfonyl)imide (LiTFSI) in 1,3-dioxolane/1,2-dimethoxymethane (DOL/DME, 1:1 by volume) (Zhangjiagang Guotaihuarong New Chemical Materials Co., Ltd.). Galvanostatic discharge/charge voltage profiles of the assembled cells were performed on an

LAND system at 0.1 C (1 C = 1675 mA g^{-1}, based on S) in the voltage range of 1.0–2.7 V (vs. Li^+/Li) in the first three cycles and 1.1–2.7 V (vs. Li^+/Li) in the following cycles. Galvanostatic intermittent titration technique (GITT) was applied to determine the quasi-equilibrium reduction potential. For GITT measurement, the cell was discharged at 0.1 C for 30 min, followed by relaxation for 10 h. The procedure of discharge-relaxation was repeated until the voltage reached 1.2 V. The C-rate used is based on the theoretical capacity of S (1675 mA h g^{-1}). Cyclic voltammogram (CV) test was carried out using an Autolab PG302N electrochemical workstation from 1.0 to 2.7 V (vs. Li^+/Li) at a sweep rate of 0.1 mV/s. All electrochemical measurements were carried out at 25 °C.

***Ex situ* and *in situ* measurement**

Ex situ characterizations were applied to gain the information of structure evolution of S/CNTs during lithiation and delithiation. Swagelok-type batteries of S/CNTs in different discharge/charge states were disassembled in the glove box. The electrodes were washed by DOL and DME to remove the electrolyte and residual LiTFSI prior to characterization unless otherwise noted. The electrodes were then transferred to special designed devices for ex situ SEM, EDX, XRD, Raman, and XPS analyses. For ex situ TEM observation, the S/CNT electrode washed by DOL and DME was first immersed in NMP solvent in an Ar-sealed tube and then sonicated to dissolve the binder and get well dispersed S/CNTs. In situ Raman spectra were collected simultaneously with CV test, using a special designed stainless steel cell with a small transparent window.

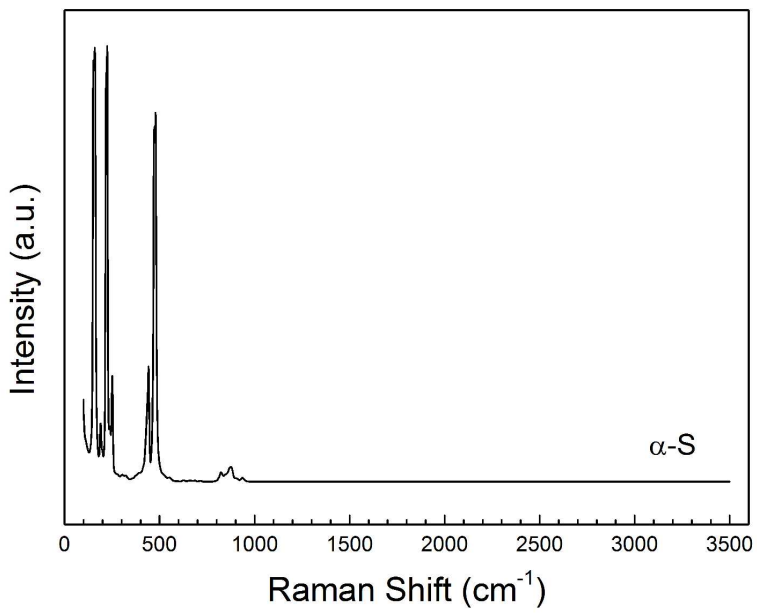

Figure S1. Raman spectrum of α-S.

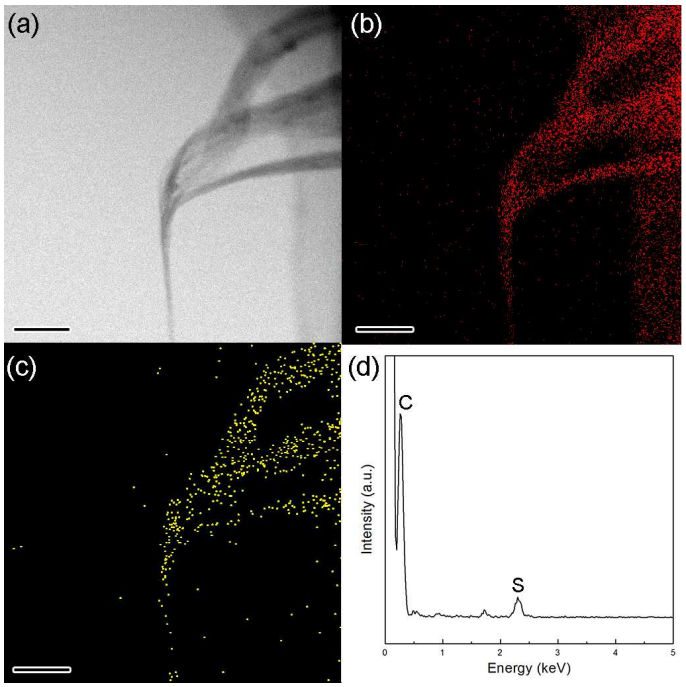

Figure S2. (a) STEM image, (b) C elemental mapping, and (c) S elemental mapping of S/CNTs (scale bar: 100 nm); (d) EDX spectrum collected from the center of STEM image in (a).

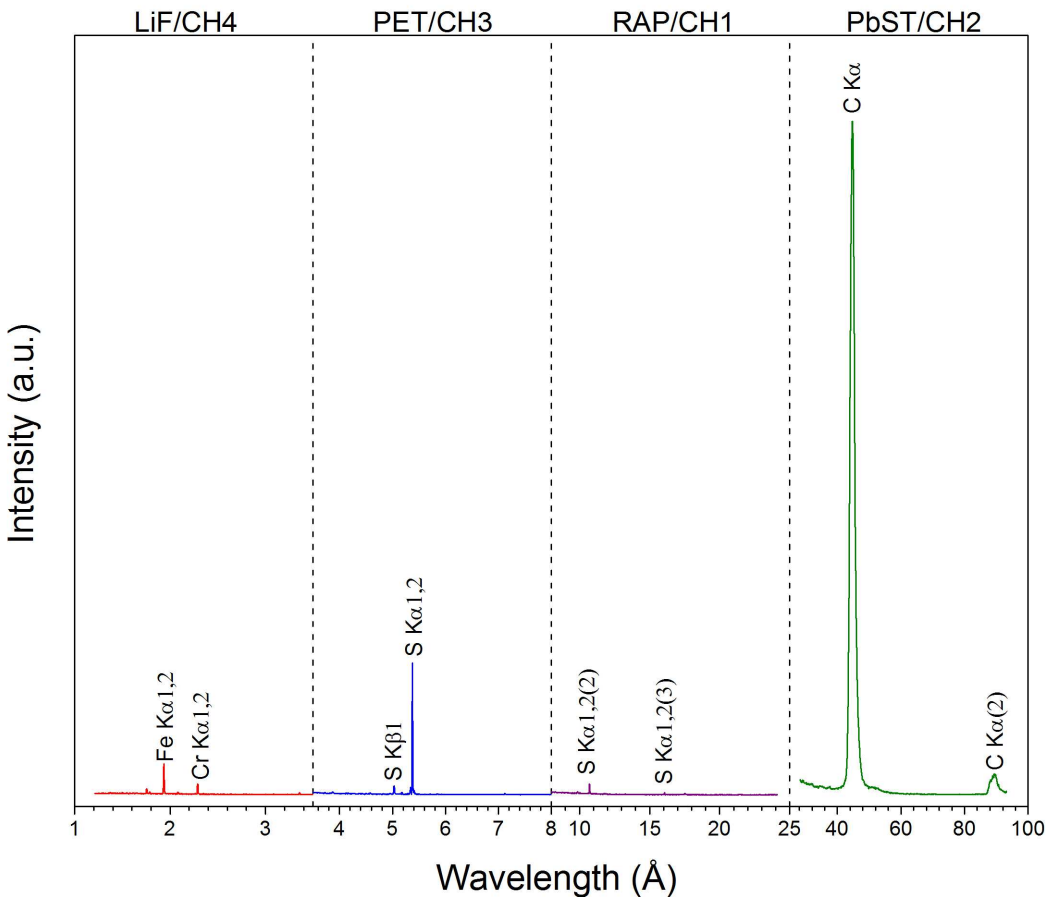

Figure S3. Wavelength dispersive X-ray spectrum of S/CNTs.

Quantitative analysis by comparing the collected elemental signals of S/CNTs and standard samples on EPMA shows the S content in S/CNTs is 10.6 wt%.

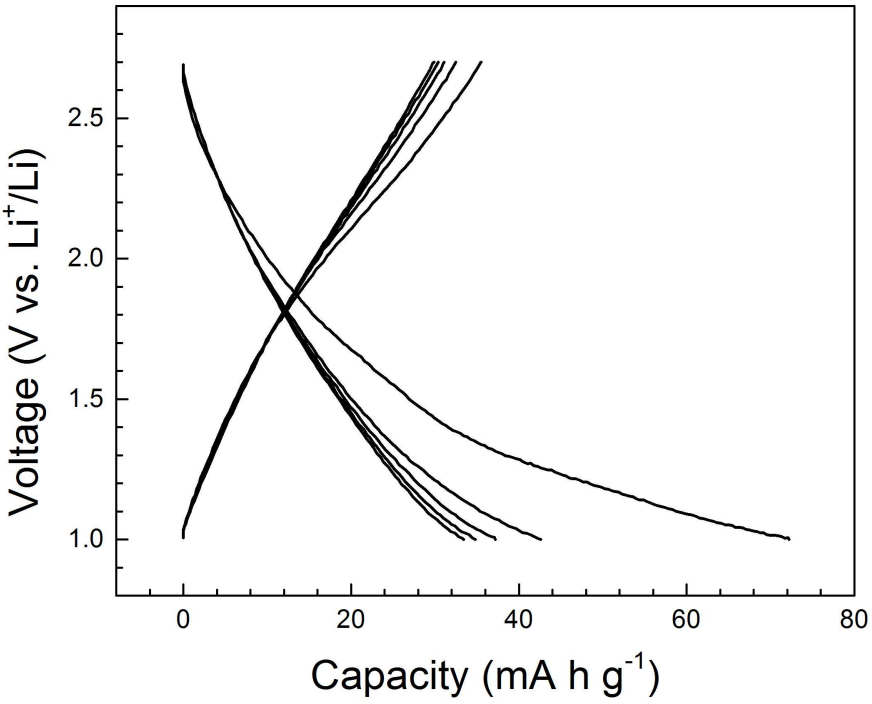

Figure S4. Galvanostatic discharge/charge voltage profiles of empty CNTs.

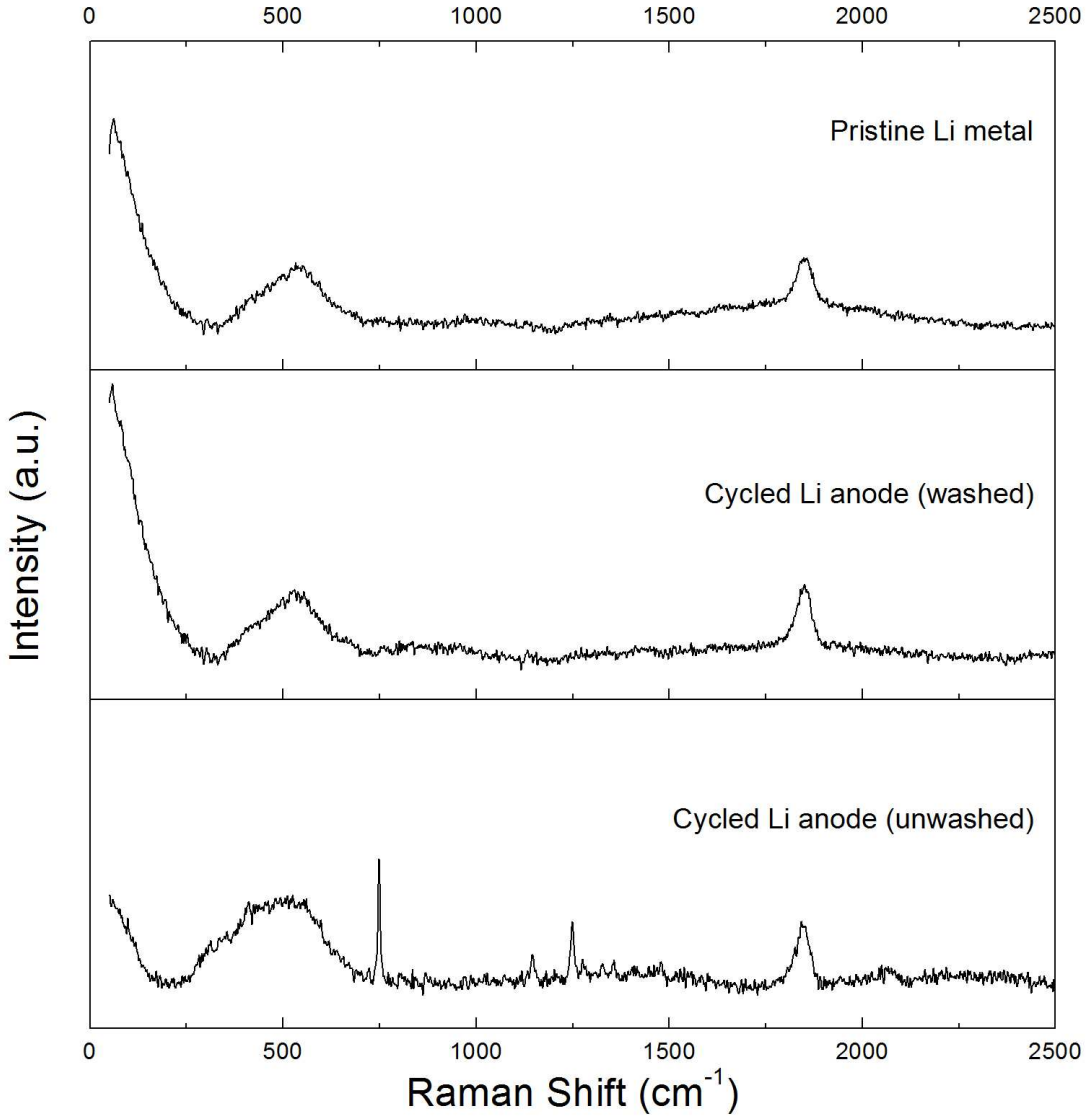

Figure S5. Raman spectra of pristine Li metal and Li anodes (washed by DOL/DME or unwashed) after 10 cycles.

Raman spectra of cycled Li are similar to that of the pristine Li, except for some peaks of Li salt on the unwashed Li anode. Raman signal of Li_2S (see Figure S13), which has a sharp and strong peak at 375 cm^{-1}, is not detected on the cycled Li anode. The Raman spectra on the Li anode further evidence that the S species are not transported to the anode.

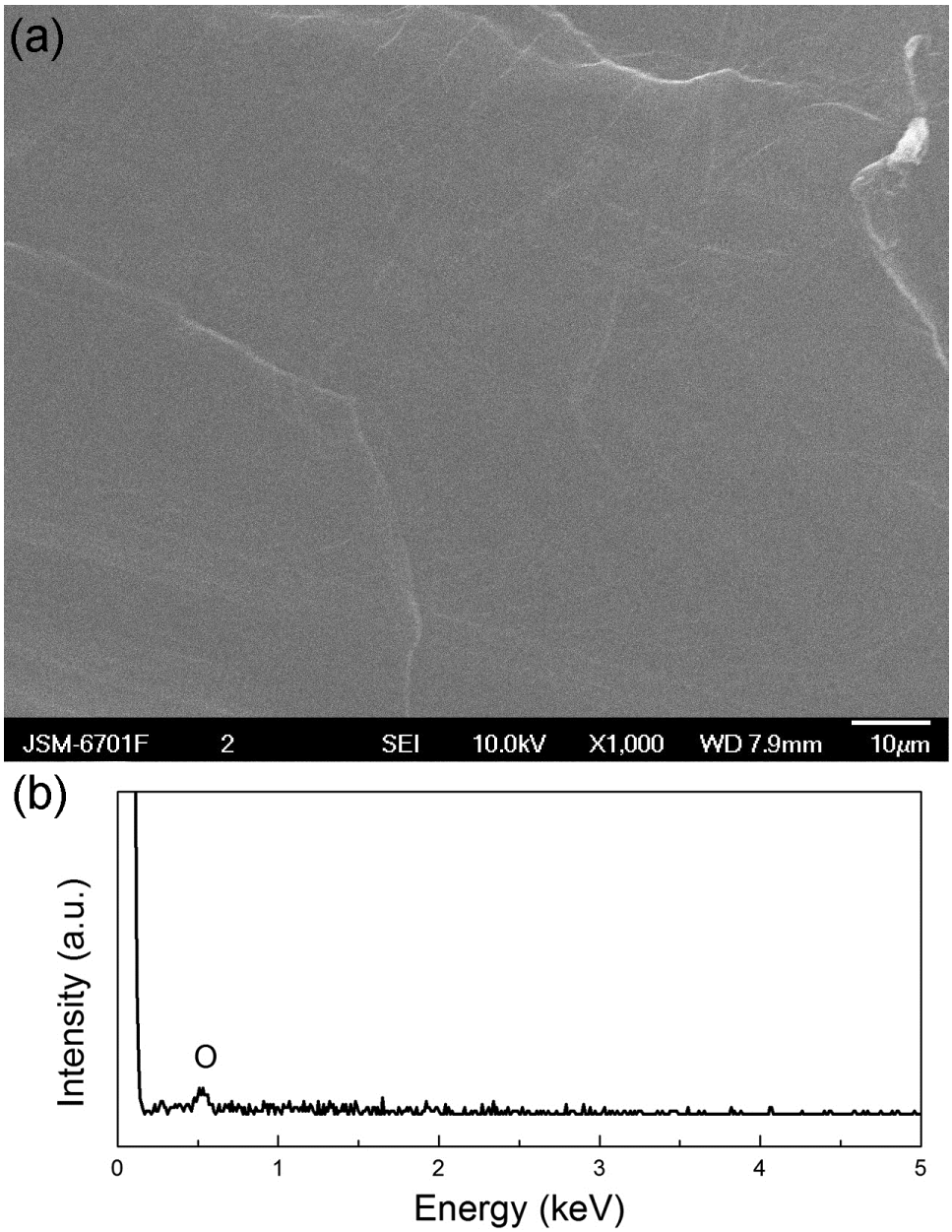

Figure S6. (a) SEM image and (b) EDX spectrum of the cycled Li anode after 10 cycles (washed by DOL/DME).

The Li anode after cycling (washed by DOL/DME) shows a clean surface without Li_2S particles deposited. EDX signal of S are not identified, indicating that no S species are migrated to anode. SEM observation and EDX spectrum collection for the unwashed Li anode is significantly affected by residual LiTFSI salt and are thus not shown.

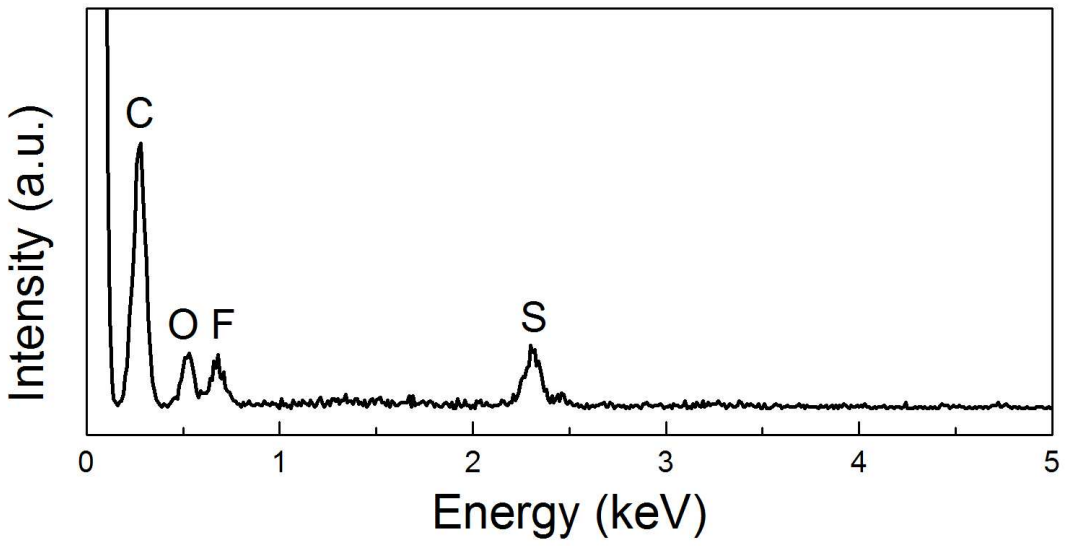

Figure S7. EDX spectrum of a cathode disassembled and repeatedly washed by DOL/DME after 10 cycles.

According to the EDX spectrum, S is obviously observed on the cycled cathode and its weight ratio is ~8% (including the PVDF binder on the cathode), approaching the pristine ratio. The EDX result evidences the S retention on the cathode after cycling.

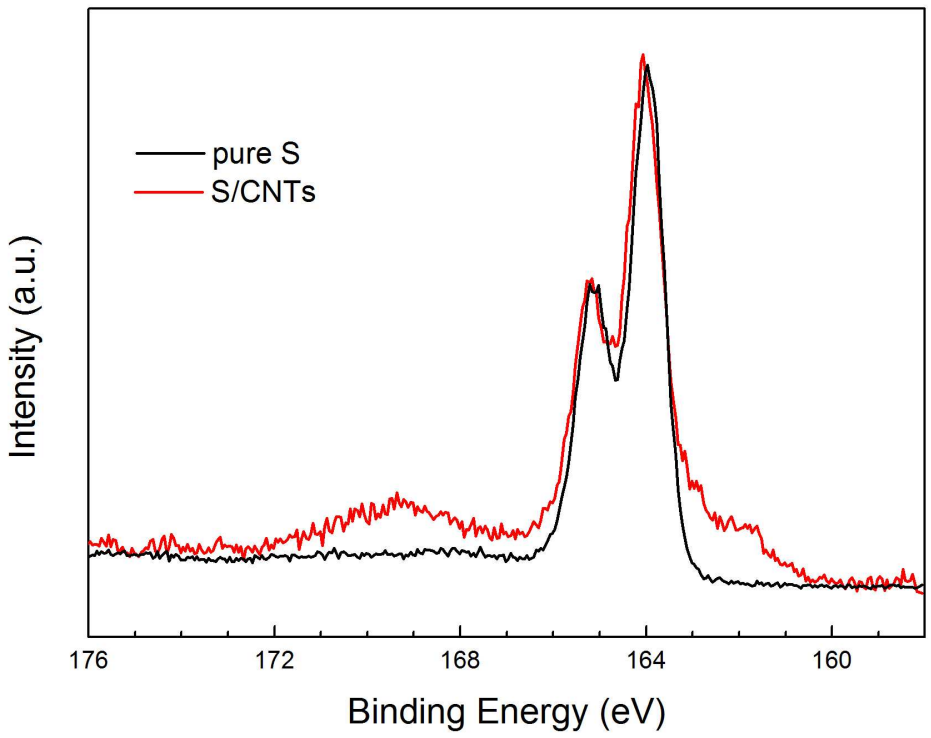

Figure S8. XPS S 2p spectra of pure S and pristine S/CNTs. The intensity has been normalized.

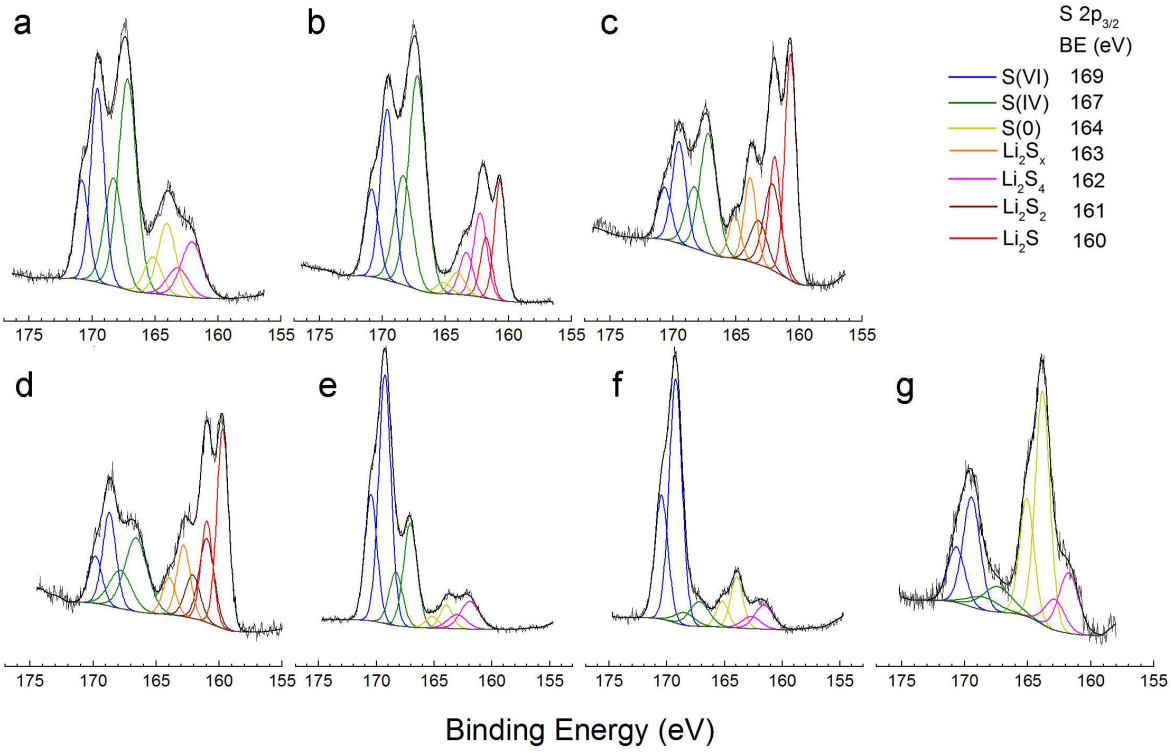

Figure S9. Ex situ XPS spectra of S $2p_{3/2}$ in S/CNTs in different DoR (a–g corresponding to point a–g in Figure 4a).

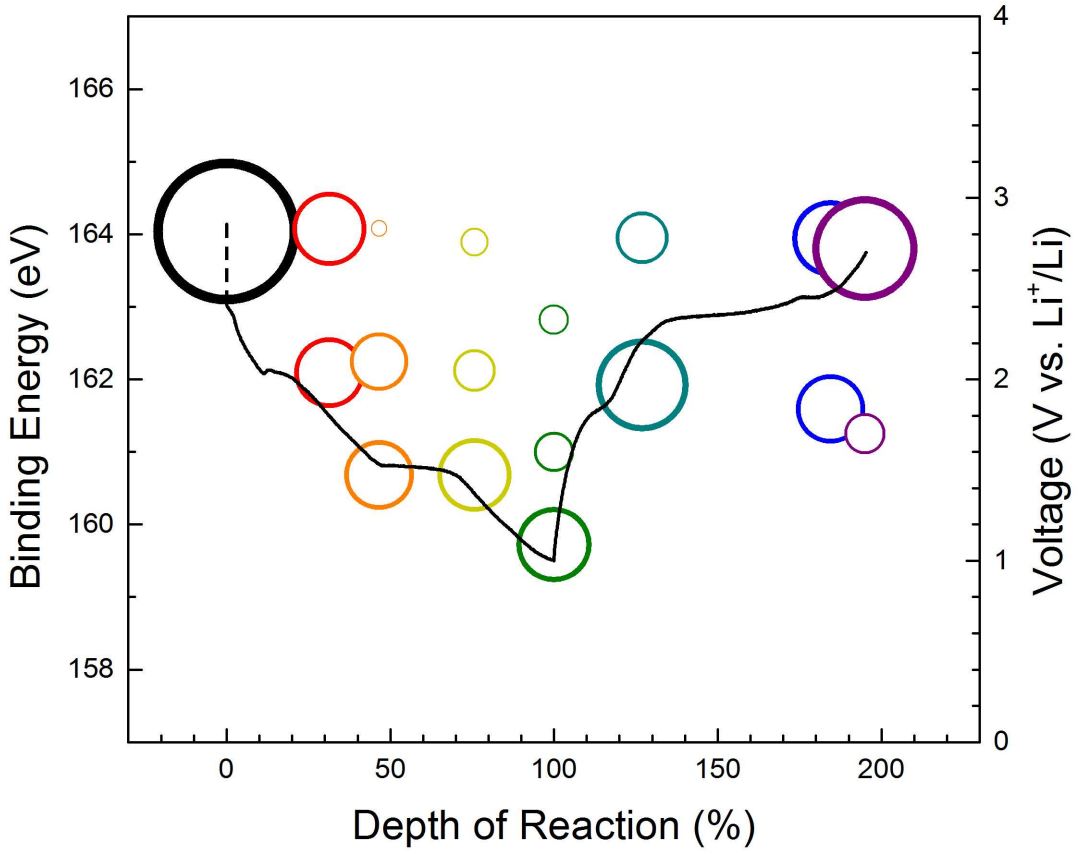

Figure S10. Evolution of the binding energy of S $2p_{3/2}$ in S species (colored bubble) with discharge/charge reaction (black line). For each DoR, the S species are shown by bubble(s) with a specific color. The y-coordinate of the bubbles shows the binding energies of the corresponding S species; the area is mapped from the ratio of corresponding species (by XPS peak fitted in Figure S9).

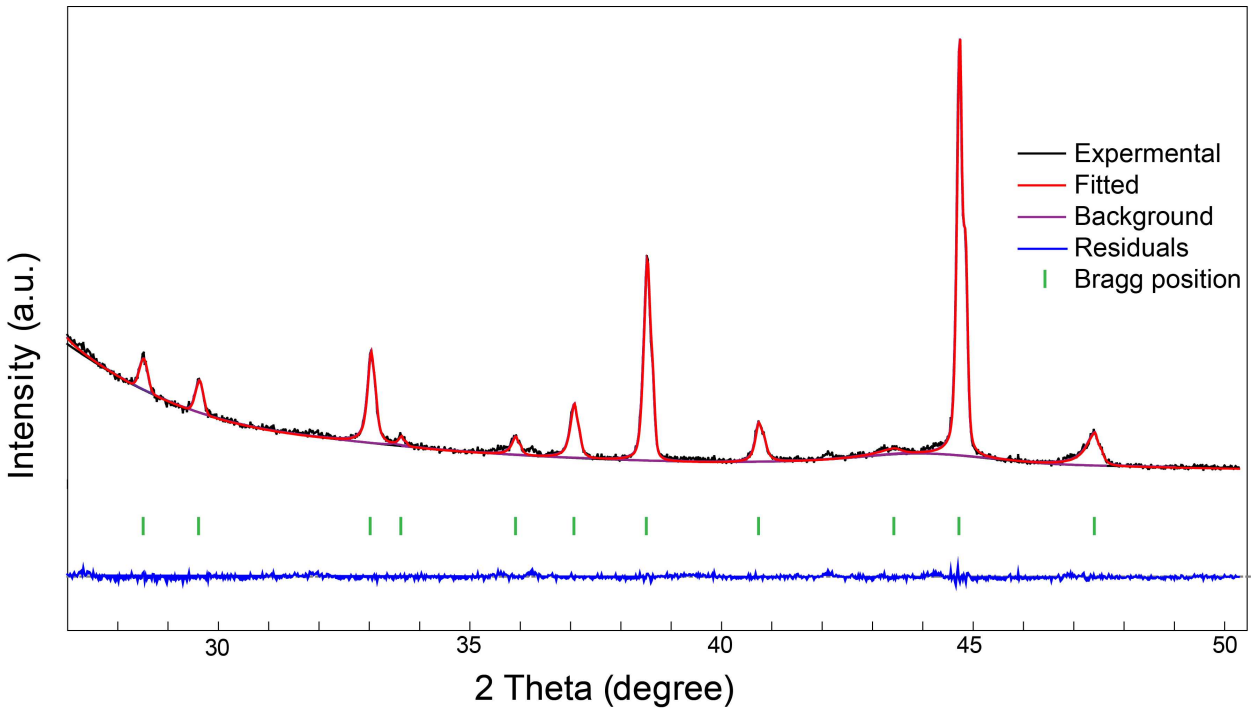

Figure S11. Refinement of the XRD pattern of S/CNTs electrode (with Al foil) before electrochemical test (point o in Figure 4a).

A series of refinement for electrode during cycling (profiles a–g in Figure 4b) are made by the same method here. The results of refinement disclosing the *d*-spacing and domain size of the linear chains, as well as the errors given by the refinement, and are shown in Figure 4c.

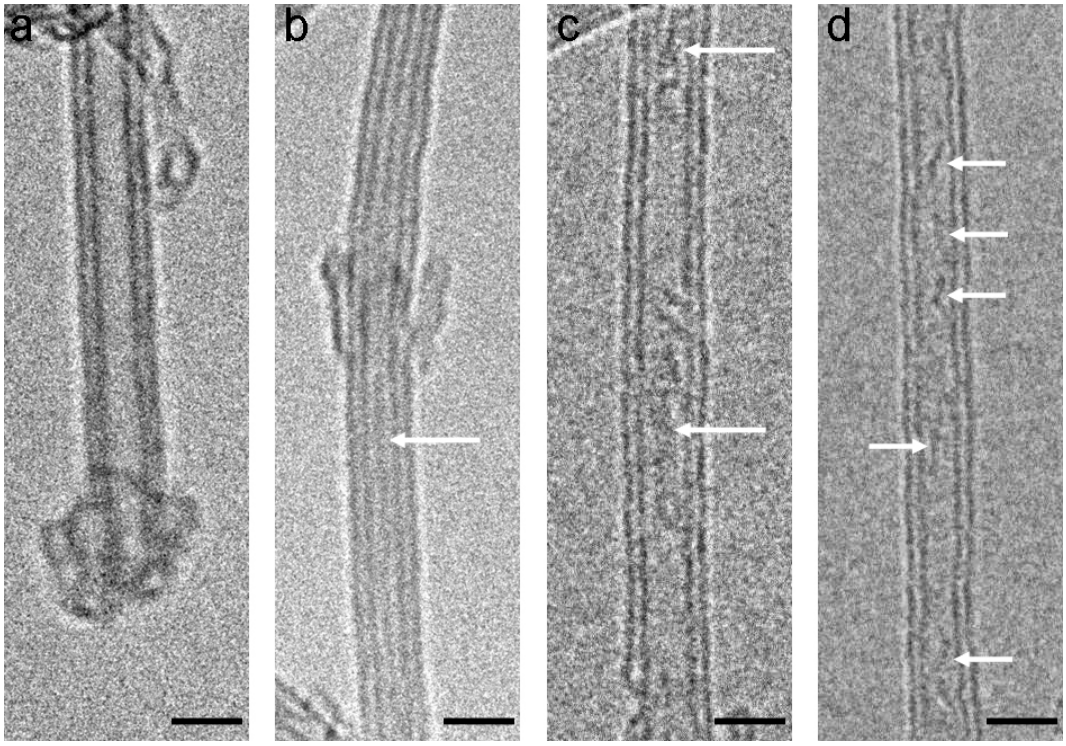

Figure S12. TEM images of (a) an empty open-ended DWCNT, (b) a linear S chain in DWCNT, (c) short S chains in DWCNT after one cycle, and (d) shorter S chains in DWCNT after 10 cycles (scale bar: 2 nm). S chains are indicated by the arrows. We note that there is some amorphous carbon outside the CNTs in panels a and b because of the open-ending process.

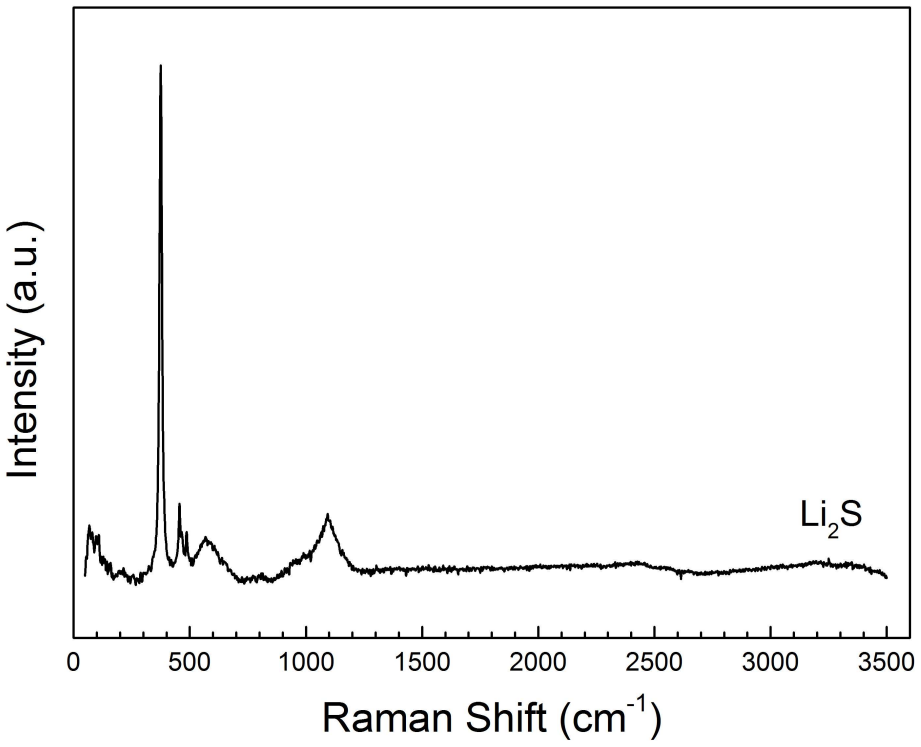

Figure S13. Raman spectrum of commercial Li_2S.

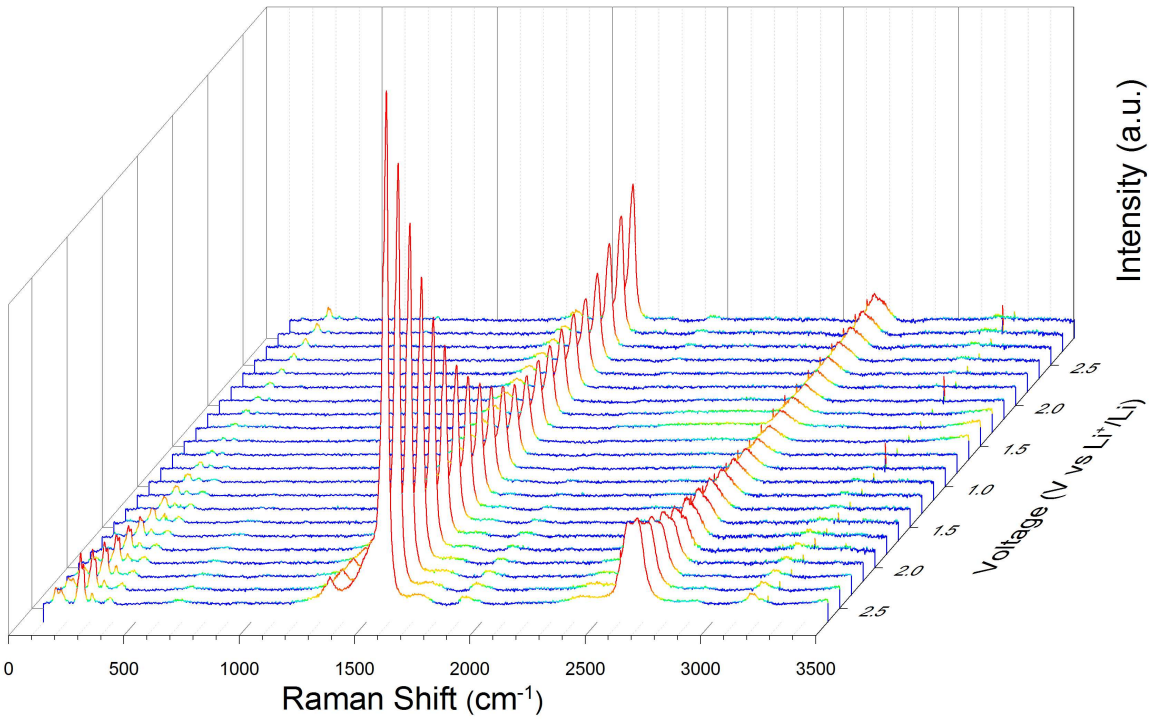

Figure S14. In situ Raman spectra in the range of 100–3500 cm^{-1} during the initial cycle of S/CNTs.

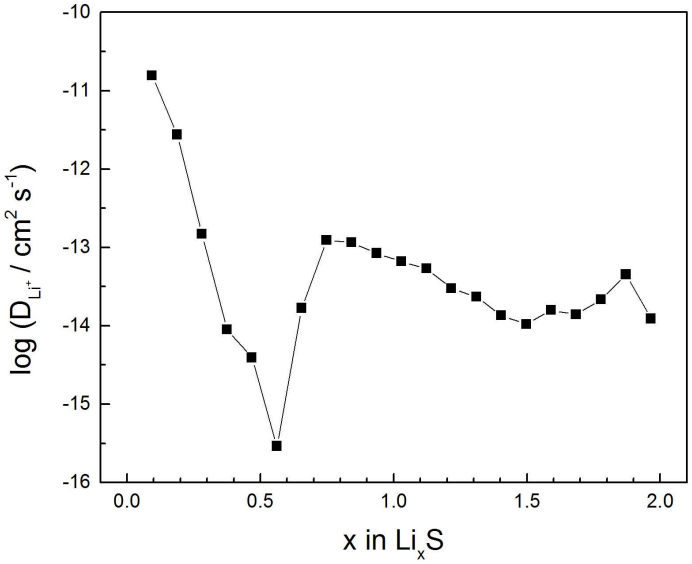

Figure S15. Chemical diffusion coefficient of Li^+ in the initial discharge of S/CNTs derived from the GITT data.

We calculated the chemical diffusion coefficient of Li^+ ($\tilde{D}_{Li^+}$) in the initial discharge of S/CNTs according to the GITT data in Figure 2c.[1] $\tilde{D}_{Li^+}$ is plotted as the function of x in Li_xS. Diffusion of Li^+ is relatively easy at the beginning, but becomes difficult as more Li^+ is intercalated in S chains. At $x \approx 0.5$, diffusion of Li^+ is the slowest. This is because Li^+ ions first react with S chains forming Li_2S_4. It is first easy and fast to react with the terminal several S atoms of S chains so that the over potential is small. The lithiation becomes difficult when the reaction takes place into the interior of S chains because many Li^+ ions have already occupied the diffusion path, resulting in a large over potential of 0.3 V. In the lithiation process afterwards, $\tilde{D}_{Li^+}$ is stable at 10^{-13}–10^{-14} cm^2 s^{-1}.

REFERENCE

(1) Tang, K.; Yu, X.; Sun, J.; Li, H.; Huang, X. *Electrochim. Acta* **2011**, *56*, 4869.